CHAPTER-3

An Advanced Micromagnetic Simulation Framework Enabled by NEGF Formalism for Modeling of STT-MTJ Devices

The part of the work is adopted from-

J. Rajpoot and S. Verma, "An Advanced Micromagnetic Simulation Framework Enabled by NEGF Formalism for Modeling of STT-MTJ Devices," ***IEEE Transactions on Magnetics***, July 2024, (**Under revision**).

Abstract:

In the modern era, when non-volatile memory is gaining a lot of attention, spin transfer torque magnetoresistive random access memories (STT-MRAM) have emerged as a promising technology, offering fast access and the capability to implement in-memory and neuromorphic computing architecture. This emphasizes the necessity to explore the STT switching process to utilize its maximum potential in data storage and novel computing applications. Considering this, researchers have developed embedded micromagnetic simulation frameworks using an object-oriented micromagnetic framework (OOMMF) evolver extension module for a comprehensive analysis of the STT-MTJ switching process. However, they do not offer an appropriate spin transport module for an accurate picture of STT-MTJ devices. To address this gap, we present an advanced micromagnetic simulation framework enabled by the non-equilibrium Green's function (NEGF) formalism for the modeling of STT-MTJ devices. It uniquely combines the NEGF model scripted in tool command language (TCL) for spin transport and the micromagnetic simulations for magnetization dynamics. The proposed framework facilitates in-depth analyses of the STT switching behaviour in MTJs. In the proposed approach, micromagnetic simulations are performed by updating the critical parameters of the MTJ derived from the spin transport model. Further, non-uniform current density (NUCD) distribution is incorporated to enhance the accuracy and capability of the proposed framework. This framework ensures a more accurate picture of the STT switching process, paving the way to optimize the STT-MTJ devices for practical applications in non-volatile memory and novel computing systems.

3.1 Introduction

With the rising demand for fast and more energy-efficient memory solutions, spin transfer torque magnetoresistive random access memories (STT-MRAM) have emerged as potential choices for next-generation non-volatile memory [111]. Therefore, a detailed investigation of the spin transport and magnetization dynamic in magnetic tunnel junctions (MTJs) is crucial for realizing their maximum potential in revolutionizing memory storage and computing capabilities [29], [112]. The MTJ devices have a complex architecture that needs to be analyzed in a micromagnetic simulator, which has the closest existing solvers that aid the simulation of magnetization dynamics in MTJ devices. The existing micromagnetic simulation frameworks for MTJs capture magnetization dynamics while considering that the current density does not depend on the relative alignment of the spin configuration of free and pinned layers during the magnetization switching. However, during the switching process, spin configurations vary from point to point, which leads to a change in the resistance of the MTJ. Consequently, the current density through the MTJ structure experiences variations rather than being constant, particularly in the case of high TMR MTJs [113]. Further, S. Fiorentini *et al*. reported that current density can vary by a factor of three in modern MTJ devices, where the TMR is greater than 200 % [114]. Moreover, C. Y. You *et al*. [115], [116] focused on advancing an OOMMF extension module for a more flexible micromagnetic simulation, illustrating the TMR-dependent switching process with NUCD. However, they do not offer an appropriate spin transport module for an accurate picture of STT-MTJ devices. Datta *et al*. [117] reported a non-equilibrium green function (NEGF) based spin transport model to calculate the spin conductance and the spin torque of MTJ devices. Also, their coupled model allows us to estimate experimental switching voltage for the antiparallel (AP) to parallel (P)

and P to AP switching employing various MTJ devices and material parameters related to the ferromagnet and dielectric. However, these models do not have the capability to analyze the magnetization dynamics in the free layer (FL) of the MTJ. Also, the spin transport model based on NEGF formalism does not incorporate the NUCD effect, which has a significant impact on magnetization dynamics or the switching behaviour of MTJ devices.

The micromagnetic simulation tools, such as OOMMF [108] and Mumax3 [109], are widely considered for capturing the magnetization dynamics or switching behaviour of the MTJ. These tools incorporate state-of-the-art solvers that effectively modeled the magnetization dynamics. Also, several OOMMF extension modules proposed by various research groups from both academia and industry are available in the open source [118]. However, they do not offer an appropriate spin transport module for an accurate picture of MTJ devices. Hence, the MTJ design is handled using a mixed-mode simulation framework consisting of magnetization dynamics [95], [117], [119], and the spin transport model based on NEGF formalism is considered separately. Further, Jullière's model [33] for spin transport and monodomain approximation for magnetization dynamics are used in compact models [120], [121], [122], [123], [124], [125], [126], [127], [128] compatible with SPICE.

The discussion in this section so far delineates the lack of capability of existing simulation frameworks and tools to simultaneously incorporate spin transport and magnetization dynamics using the physical and materials parameters of ferromagnetic (FM) and non-magnetic (NM) material. To address this gap, we present an advanced micromagnetic simulation framework enabled by the NEGF formalism for the modeling of STT-MTJ devices. It uniquely combines the NEGF model scripted in tool command language (TCL) for spin transport [117] and the micromagnetic simulations for magnetization dynamics [108]. The

proposed framework facilitates in-depth analyses of the MTJ device by calculating the crucial parameters, such as magnetoresistance, in-plane torque (STT) and out-of-plane torque or field-like torque (FLT) components of the spin torque, and spin torque efficiency terms through the spin transport model. These crucial parameters are employed in the micromagnetic simulation to capture the magnetization dynamics accurately while also considering the NUCD effect. In this approach, micromagnetic simulations are performed using the OOMMF tool, which is invoked repeatedly within the main Python script for a short time (Δt). The main Python script continually re-executes the input file, updating the critical parameters from each preceding simulation step until the entire simulation period is completed. As a result, NUCD and uniform current density (UCD) distribution during the magnetization switching are shown to demonstrate the accuracy and capability of the proposed framework. This framework ensures a more accurate picture of the STT switching process, paving the way to optimize the STT-MTJ devices for practical applications in non-volatile memory and novel computing systems.

3.2 MTJ Device Physics Behind the Simulation Framework

The MTJ device is a multi-layered structure, which is composed of a thin MgO layer sandwiched in between the ferromagnetic (FM) layers called a pinned layer (PL) and a free layer (FL), as shown in **Figure 3.1**. The ferromagnetic layers have perpendicular-plane anisotropy. Here, it is assumed that electronic transport occurs along the z-direction, whereas the magnetization of the FM layers is in the x-y plane. The magnetization of the PL is assumed to be along the z-direction, whereas the magnetization of FL is confined in the x-y plane, making an angle θ with the z-direction. In the modern era, spin-transfer torque (STT) switching has become the predominant mechanism for magnetization reversal. This mechanism enables

magnetization switching without the use of external magnetic fields and offers promising device applications. The magnetization switching is accomplished due to a spin-polarized current flow from the PL, exerting torques (current-induced torques) on the FL or vice versa. The STT combines the in-plane (Slonczewski's torque) and out-of-plane (field-like torque) torque components. Various existing simulation framework ignores the impact of FLT on switching [115]. However, the efficiency of the FLT is negligible for the spin valves but lies between 10 % to 100 % for MTJs [182]. Therefore, FLT has also been incorporated into the proposed framework.

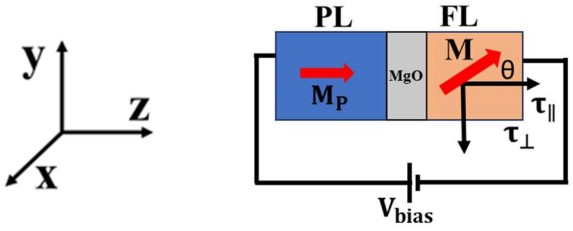

Figure 3.1 Schematic representation of the STT-MTJ device under applied bias voltage (V_{bias}). It also shows that the magnetization of the PL is M_P along the z-axis and of the FL is M, which makes an angle θ with the z-axis.

3.2.1. NEGF Formalism for Spin Transport

The spin transport model based on NEGF formalism is used in the proposed framework to analyze the charge and spin conductance in STT-MTJ, as discussed in the literature [117], [119]. The same spin transport model is currently being used in commercial Sentaurus device simulator, as detailed in its user document [183]. In this work, we have adopted the same spin transport model, which is based on the NEGF formalism, by developing a TCL script in accordance with the model presented in the thesis [184] which is shown to be precise in their calculation of spin conductance and torque components. Here, the charge and spin current densities are evaluated based on the Hamiltonian approach, as reported in the literature [117]. The in-plane and out-of-plane components of the spin torque exerted on the FL are expressed

by

$$\overrightarrow{\tau_{||}} = \frac{\overrightarrow{I_S}.(M \times M_P \times M)}{(1-(M.M_P)^2)} \quad 3.1$$

$$\overrightarrow{\tau_{\perp}} = \frac{\overrightarrow{I_S}.(M \times M_P)}{(1-(M.M_P)^2)} \quad 3.2$$

where, $\overrightarrow{I_S}$ is represents the spin current, and M and M_P denote the unit vector in the direction of magnetization in the FL and PL, respectively.

Table 3.1 Summary of Parameters Used in the Spin Transport Model of MTJ

Parameter	**Symbol**	**Value**
FM effective mass	m^*_{FM}	0.38
Insulator effective mass	m^*_{OX}	0.16
Barrier height	E_b	0.76 eV
Equilibrium Fermi level	E_f	2.25 eV
Oxide thickness	t_{ox}	1.1 nm
Area of FL	S	11600 nm^2
FL thickness	t_{FM}	2 nm
Spin splitting	Δ	2.15 eV
Saturation magnetization	M_S	800 emu/cm^3
Uniaxial anisotropy	K_{U2}	$2.42e^4$ emu/cm^3
Gilbert damping parameter	α	0.01
Voltage range	V	[-0.5V, 0.5V]

The bias dependence of in-plane and out-of-plane spin torque components and their efficiency terms is a crucial point to be considered during the magnetization switching in the MTJ devices that impacts magnetization dynamics [120]. Therefore, we used the spin transport model based on NEGF formalism to achieve more accurate and precise calculations of the spin torque and magnetoresistance in the MTJ with respect to the bias voltage. To integrate this model with micromagnetic simulations in the proposed framework, we developed a TCL script for the spin transport model based on the MATLAB code, which is presented in the thesis [184]. This approach facilitates seamless incorporation of the model with the OOMMF tool. Furthermore, validation of the developed TCL script is conducted with MATLAB results [184] and experimental data cited in the literature [119] using MTJ

parameters listed in **Table 3.1**. We observed that the results obtained from the TCL script closely replicate both MATLAB and experimental findings, as demonstrated in **Figure 3.2** and **Figure 3.3**, respectively.

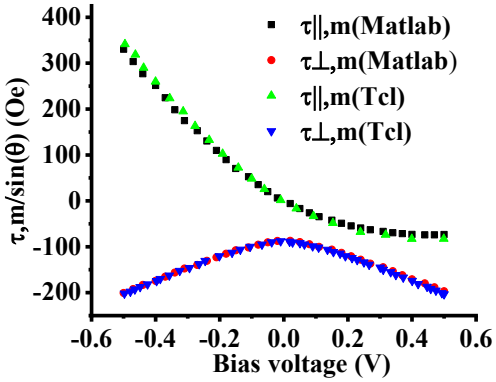

Figure 3.2 Illustration of spin transfer torque components with respect to bias voltage across the MTJ: (a) In-plane torque (τ||,m) and (b) Out-of-plane torque (τ⊥,m).

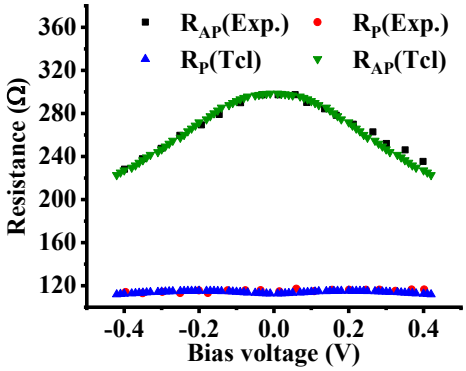

Figure 3.3 Demonstration of the MTJ resistance with the applied bias voltage and validation of the model scripted in the TCL with the experimental data [119].

3.2.2. Magnetization Dynamics of Ferromagnet

To analyze the magnetization dynamics or switching in the MTJ, micromagnetic simulation using the OOMMF or Mumax3 needs to be performed. The OOMMF tool has an inbuilt model of the MTJ for 0K [108]. OOMMF evolvers are also available as open sources that incorporate thermal fluctuation in STT switching [118]. In these evolvers, the magnetization dynamics of FL in response to STT generated by PL are determined from the Landau-Lifshitz-Gilbert-Slonczewski (LLGS) equation stated as follows:

$$\frac{dM}{dt} = -\gamma\left(M \times H_{eff}\right) + \alpha\left(M \times \frac{dM}{dt}\right) - \tau_{ST} \quad 3.3$$

where, M represents the unit vector in the direction of magnetization under the influence of spin torque (τ_{ST}) in the FL, γ is the gyromagnetic ratio, and α is the damping constant. H_{eff} is the effective field, which is the vector sum of the external magnetic field, exchange field, demagnetizing field, anisotropy field, and thermal field. Where, the thermally field captures the stochastic thermal noise effect at finite temperatures. Here, Slonczewski's model is utilized to implement the spin torque, which combines the in-plane (STT) and out-of-plane (FLT) torque components, as reported in [182]. However, this model does not include the dependence of FLT on the bias current density (or voltage). Another study that was presented in [185] for STT dynamics shows that the FLT varies quadratically with the current density. The spin torque (τ_{ST}) used in the model [185] is stated as follows:

$$\tau_{ST} = |\gamma|\beta \in (M \times M_P \times M) - |\gamma|\beta \in' (M \times M_P) \quad 3.4$$

$$\beta = \left|\frac{\bar{h}}{\mu_0 e}\right| \frac{J}{t_{FL} M_s} \quad 3.5$$

$$\in = \frac{P\Lambda^2}{(\Lambda^2+1)+(\Lambda^2-1)(M.M_P)} \quad 3.6$$

or alternatively, $$\in' = \eta_{FLT} \in \quad 3.7$$

where, $\in$ and $\in'$ are the spin torque efficiency terms, which depend on the magnetization alignment of FL and PL, as well as spin polarization (P) and lambda (Λ) as expressed in equation (3.6). In the definition of β, e is the electron charge in C, J is the current density in A/m^2, t_{FL} is the thickness of the FL in meters, and M_s is the saturation magnetization in A/m. η_{FLT} is the efficiency of the FLT that lies between 10 % to 100 % of STT for the MTJs reported in [182]. Therefore, the FLT cannot be neglected while using the LLGS equation in the case of the MTJs.

3.2.3. Non-Uniform Current Density (NUCD) Profile

During the switching process, spin configuration varies from point to point in the FL, which leads to a change in the resistance of the MTJ. This change in the resistance is attributed to the relative alignment of spin configuration within the free and pinned layers. Consequently, the current density flowing through the MTJ structure experiences variations rather than remaining constant throughout the magnetization switching process. To tackle this challenge, D. Aurélio *et al*. [113] conducted a micromagnetic investigation for the STT magnetization switching considering the non-uniform current density (NUCD) distribution in the high-TMR MTJs. Their analytical expressions facilitate the calculation of current density, considering the NUCD effect.

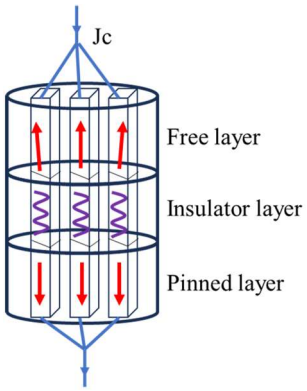

Figure 3.4 Finite elements in the MTJ with the resistance of the unit cell

This work implements the NUCD profile by employing a parallel resistance channel model, as shown in **Figure 3.4**. For this implementation, we have meshed the MTJ with a cross-section area of S into finite small unit cells, each having a cross-section area of ΔS. The resistance of each parallel channel for parallel and anti-parallel configuration is estimated by dividing the MTJ resistance by the number of unit cells ($N = S/\Delta S$). The estimated resistance of each parallel channel for parallel configuration is $R'_P = R_P/N$, and for anti-parallel configuration $R'_{AP} = R_{AP}/N$. The resistance of each parallel channel (i, j), denoted as

$R\ (i,j)$, depends on the relative alignment of spin configuration or the normalized magnetization vectors of both the FL and PL. This resistance is calculated using the following expression

$$R(i,j) = R'_P + \left(\frac{R'_{AP}-R'_P}{2}\right)(1 - M(i,j).M_P(i,j)) \quad 3.8$$

where, R'_P and R'_{AP} represent the resistance of each parallel channel in the P and AP states, respectively. $cos\theta = M(i,j).M_P(i,j)$ represents the dot product of the normalized magnetization vectors of both the FL and the PL of each unit cell (i,j). To estimate the current density of each channel, we assume that the tunneling current flows only in the vertical direction from the (i,j) unit cell of the FL to the (i,j) unit cell of the PL or vice versa. Therefore, the current density flow through each cell is estimated as

$$J(i,j) \ = \frac{V_{mtj}}{R(i,j)\times\Delta S} \quad 3.9$$

where, $J(i,j)$ represents the current density for each cell (i,j). It also depends on the spin configuration of the FL. The estimated current density of each parallel channel is updated into the input file of the micromagnetic simulation at each small time (Δt) step.

3.3 Results and Discussion

This section showcases the effectiveness of the proposed framework using an MTJ with an area of 1256 nm² and a FL thickness of 2 nm, along with other parameters listed in **Table 3.1** and **Table 3.2**. The simulation framework for addressing the simulation of the STT-MTJ is detailed through a flow chart, as depicted in **Figure 3.5**. Initially, the simulation starts with the NEGF-based spin transport model that captures the critical parameters (such as parallel and antiparallel resistance of the MTJ, spin torque efficiency terms) governing switching dynamics in relation to the applied bias voltage and material properties. These critical

parameters are subsequently updated into the micromagnetic simulation input file (*.mif) created for the MTJ, which is used for micromagnetic simulation by calling the OOMMF tool for a small-time 'Δt' around 10 ps using the "bosxi" command in the main control program. The main control program is written in Python. Prior to executing the OOMMF tool for Δt time, the input (*.mif) file is updated using the critical parameter obtained from the spin transport model based on the applied voltage. At each time step of the simulation, the spin configuration file (*.omf) is called within the input file to initialize the new magnetization vector of the free layer. This new file contains the magnetization vector position of the preceding simulation step. This file serves as the initial magnetization vector position for the subsequent simulation step, ensuring continuity in the simulation process and incorporating coupled simulation of magnetization dynamics and spin transport. The output file (*.odt) is generated and continuously updated throughout the simulation.

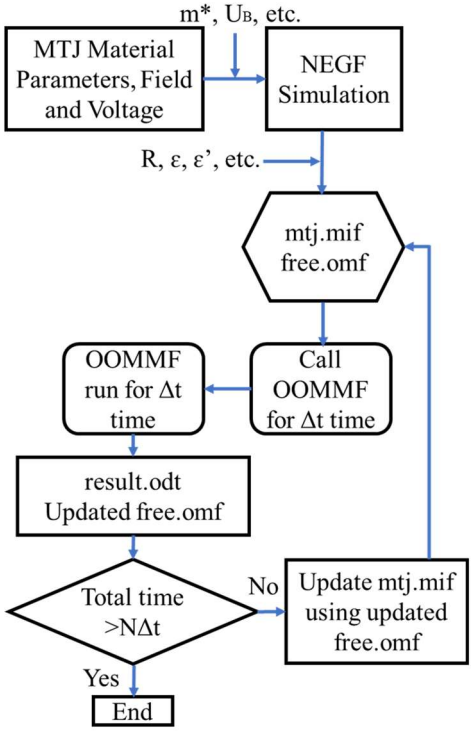

Figure 3.5 Flow chart of the simulation framework process

Table 3.2 List of Parameters Used During Micromagnetic Simulation

Parameter	Sym.	P to AP	AP to P
Sat. magnetization	M_S	0.8e6 A/m	0.8e6 A/m
Bias voltage	V	0.35 V	- 0.35 V
Parallel resistance	R_P	977.5 Ω	977.5 Ω
Antiparallel resistance	R_{AP}	2056.1 Ω	2056.1 Ω
Epsilon	∈	0.21	0.56
Epsilon prime	∈'	0.38	0.38
Lambda	Λ	1.60	1.60

3.3.1. MTJ Conductance

The spin transport model based on NEGF formalism for conductance is quite accurate and in line with experimental results compared to the Jullière *et al*. [33] model. Herein, the TCL script of the spin transport model is utilized to perform the simulation to determine the MTJ resistance with respect to a bias voltage for an area of 1256 nm^2 using the same parameter listed in **Table 3.1**, as shown in **Figure 3.6**.

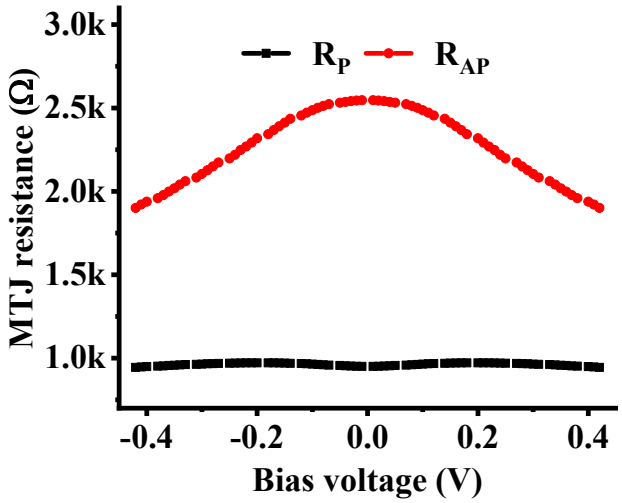

Figure 3.6 MTJ resistance demonstrates the variation with the applied bias voltage by utilizing the TCL scripted model.

3.3.2. MTJ Spin Torque Efficiency Terms

The spin torque efficiency terms (represented as ∈ and ∈′) influence the magnetization dynamics of the MTJ, where higher values lead to faster switching. These efficiency values

are determined by comparing the coefficients of in-plane ($\tau\|$) and out-of-plane ($\tau\perp$) torques from equation (3.4) with those from equations (3.1) and (3.2). The resulting values of $\in$ and $\in'$are obtained in conjunction with the bias voltage applied across the MTJ, as illustrated in **Figure 3.7**.

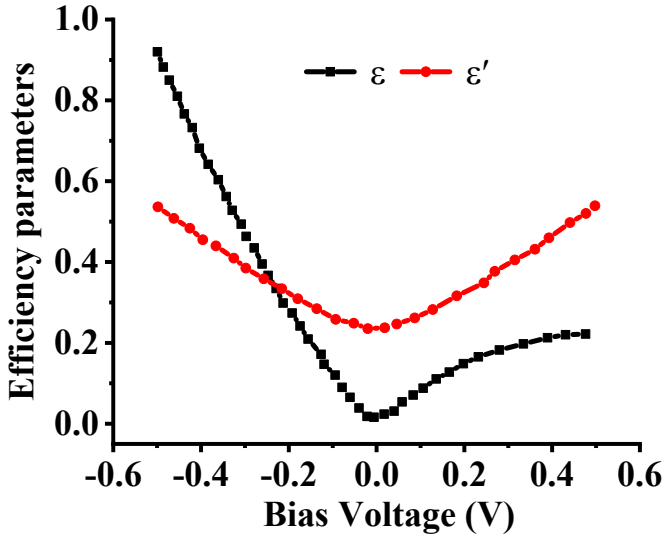

Figure 3.7 Illustration of spin torque efficiency terms (*i.e.*, $\in$ and $\in'$) in relation to the applied bias voltage across the MTJ.

3.3.3. Magnetization Switching Under Both UCD and NUCD

The existing literature reveals that the magnetoresistance is determined by the relative magnetization orientation in the free and pinned layers, which leads to changes in the current density in the MTJ during switching. In this framework, the current density is updated after every step of simulation as the magnetization orientation is obtained from the magnetization simulation in each small time of Δt, which is estimated using equation (3.8) and equation (3.9) for magnetoresistance and current density, respectively. Herein, the overall current density is estimated as

$$J_C = N \sum_{i,j} J(i,j,m) \qquad 3.10$$

To investigate the switching dynamics within the MTJ, we conducted simulations

emphasizing the switching process from AP to P and vice versa using parameters listed in **Table 3.2**, which is obtained from the spin transport model. Our observations revealed that the magnetization switching occurs more rapidly in the case of UCD compared to NUCD during AP to P switching, as depicted in **Figure 3.8(a)**. This acceleration is attributed to the reduction in current density as the switching process progresses from AP to P state, as indicated in **Figure 3.8(b)**. Conversely, when examining the P to AP switching process, as illustrated in **Figure 3.9(a)**, the magnetization switching takes a longer time in the case of UCD compared to NUCD. This difference is attributed to the current density distribution in the MTJ structure, as illustrated in **Figure 3.9(b)**.

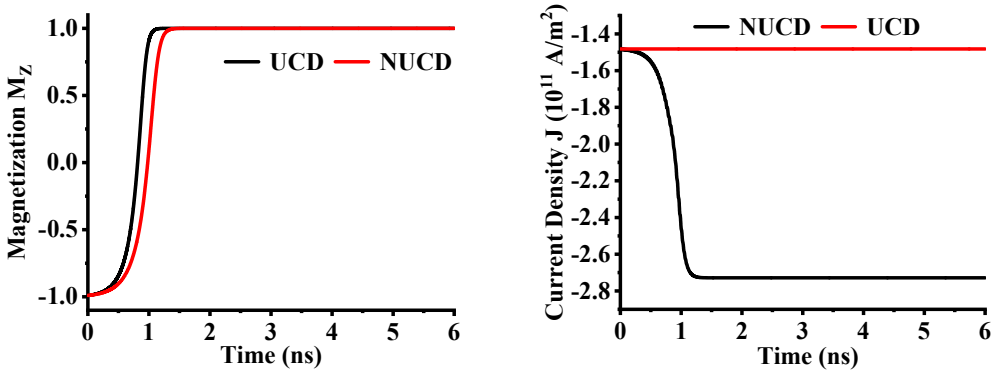

(a) (b)

Figure 3.8 Illustration of the NUCD effect and the UCD effect in the MTJ for AP to P STT switching using (a) magnetization components (M_Z) and (b) current density (J).

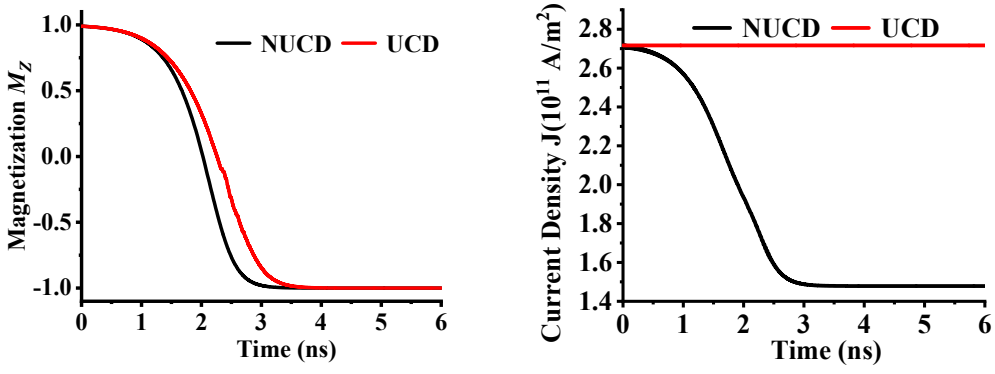

(a) (b)

Figure 3.9 Illustration of the NUCD effect and the UCD effect in the MTJ for P to AP switching using (a) magnetization components (M_Z) and (b) current density (J).

3.3.4. Study of Magnetization Switching at Different Bias Voltages

To analyze magnetization switching in MTJ under various bias voltages (*i.e.*, 0.30 V, 0.35 V, and 0.45 V), while considering NUCD effects, we conducted simulations for the P to AP switching with constant bias voltage across the MTJ throughout the switching process. The change in current density depends on the bias voltage and resistance, as defined in equation (3.9). The variations in current density at particular bias voltages directly influence magnetization switching dynamics, as depicted in **Figure 3.10**. Our observations reveal that the switching process is slowed down when a lower voltage is applied to the MTJ. This happens due to the lower current density when the low voltage is applied. Thus, switching takes relatively more time than that at higher voltage.

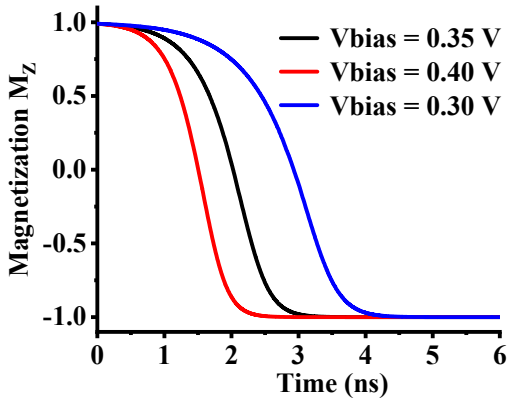

Figure 3.10 Illustration of magnetization switching of MTJ for different bias voltages.

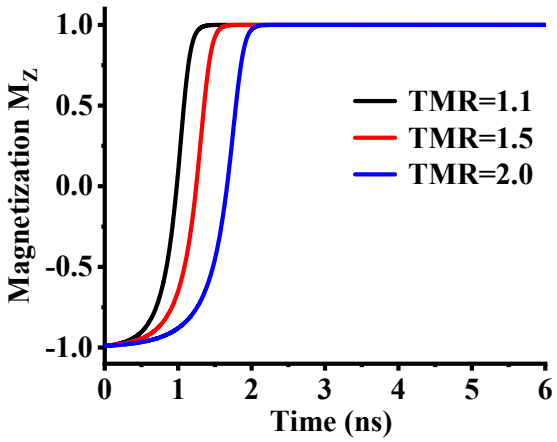

Figure 3.11 Switching behaviour with NUCD for different values of the TMR.

3.3.5. Magnetization Switching at Different TMR

To showcase the impact of TMR on NUCD switching, we conducted an analysis for AP to P switching at a fixed bias voltage of 0.35 V across various TMR values (*i.e.*, 1.1, 1.5, and 2.0) employing the NUCD switching mechanism. Our observations reveal a notable increase in the switching time as the TMR values rise, as illustrated in **Figure 3.11**.

3.4 Conclusion

In this chapter, an advanced simulation framework was developed using the micromagnetic simulation backed by the NEGF formulation of the spin-based device. Using material parameters and geometric dimensions of an MTJ device as inputs to the NEGF-based spin transport model, critical transport parameters of an MTJ device like resistance for parallel and anti-parallel states, tunneling magnetoresistance (TMR), and spin efficiency terms ($\in$ and $\in'$) are obtained. These critical spin transport parameters are used as input to the OOMMF input file for the micromagnetic simulation iteratively inside a top-level Python Script. The simulation framework is wholistic and reliable as compared to existing models and frameworks.